BMC Musculoskeletal Disorders

RESEARCH

Open Access

Risk assessment for femoral head collapse in osteonecrosis utilizing MRI-derived large lesion ratio: a retrospective cohort study

Shihua Gao[1], Haoran Zhu[2], Moshan Wen[2], Wei He[3,4*] and Ziqi Li[3,4*]

Abstract

Purpose This study aimed to developed a novel and practical method to quantify the involvement of lesion in osteonecrosis of the femoral head (ONFH). We hypothesized that the new metric large lesion ratio (LLR) had promising prognostic value.

Methods A total of 131 hips with non-traumatic ONFH were included in this retrospective study. Patient aged 18–60 with MRI-confirmed diagnosis, and a minimum of 2-year follow-up or radiographic collapse progression during follow-up were included. Patients with prior hip surgery, incomplete data or advanced ONFH at baseline (femoral head collapse > 2 mm or osteoarthritis) were excluded. Involvement of necrotic lesion was evaluated by calculating LLR. The differences of LLR between collapse progression and non-progression groups were investigated, and the differences among different scanning parameters groups were also examined. Prognostic value of LLR was examined by multivariate regression analysis. Receiver operating characteristic curves (ROC) were constructed and areas under the curve (AUC) were compared.

Results The median of LLR was 66.67% in the collapse progression group, which was significantly higher compared with 25.00% in the non-progression group ($P < 0.001$). Subgroups analysis showed that LLR were significantly higher in the collapse progression group of Japanese Investigation Committee type C1 ($P < 0.001$)and C2 ($P = 0.002$). Multivariate regression showed that LLR were independently correlated with collapse progression (OR, 1.46 [95% CI, 1.24–1.78]; $P < 0.001$). ROC analysis showed that the AUC for LLR was 0.84, outperforming the 0.74 AUC OF the JIC classification.

Conclusion LLR could served as a efficient tool to assess the risk of collapse progression and guide the selection of treatment strategy.

Keywords Osteonecrosis, Collapse, Large lesion ratio

*Correspondence:
Wei He
hw13802516062@163.com
Ziqi Li
ionsev0214@126.com
[1]Zhongshang Hospital of Traditional Chinese Medicine Affiliated to Guangzhou University of Traditional Chinese Medicine, Zhongshan, Guangdong, China
[2]Guangzhou University of Chinese Medicine, Guangzhou, Guangdong, China
[3]Traumatology and Orthopaedics Institute of Guangzhou University of Chinese Medicine, Guangzhou, Guangdong, China
[4]Department of Orthopaedics, The Third Affiliated Hospital of Guangzhou University of Chinese Medicine, No. 261, Longxi Road, Guangzhou, Guangdong, China

Introduction

Osteonecrosis of the femoral head (ONFH) predominantly affects young and middle-aged adults. ONFH often, but not always progresses into collapse of the femoral head, leading to severe hip pain and dysfunction [1, 2]. Early diagnosis and intervention has been proven to be crucial for prevention of collapse progression. It is also important to assess the risk of collapse progression in ONFH, because patients with lower risk of progression might benefit from conservative treatment, while patients with higher risk might need hip preservation surgery [3, 4].

Previous studies have established that femoral head collapse progression is closely correlated with the size and location of the necrotic lesion, and several classification systems have been developed to categorize ONFH on this basis [5–8]. Further studies suggested that the intactness of the anterior portion of the femoral head should also be paid attention to for a more comprehensive evaluation [9, 10].

Most of the methods used in current practice evaluate the necrotic lesion on radiographs or mid-coronal slice of magnetic resonance imaging (MRI) [3, 6, 11–13]. This could be problematic because the imaging information from radiographs or single slice of MRI might be insufficient to comprehensively assess the overall of necrotic lesion. Moreover, the boundary of necrotic lesion is ambiguous or even not yet appears in radiographs in some cases of early stage ONFH [14]. On the other hand, MRI has been proven to be one of the most sensitive and accurate tools in the diagnosis of early stage ONFH [2], and MRI can provide the overall image of the femoral head and necrotic lesion when taking all slices into account.

In this study, we aimed to establish and examine a novel metric named large lesion ratio (LLR) to quantify the involvement of necrotic lesion with MRI. We hypothesized that the new metric LLR had promising prognostic value.

Patients and method

Patients

This retrospective cohort study adhered to the Strengthening the Reporting of Observational Studies in Epidemiology (STROBE) guidelines and was approved by the ethics committee of the First Affiliated Hospital of Guangzhou University of Chinese Medicine (JY2023-005).

Non-traumatic ONFH patients receiving conservative treatment between January 2016 and August 2020 were reviewed retrospectively. The inclusion criteria were as follows: (1) aged 18–60 years old, (2) diagnosis confirmed by MRI, (3) and completed follow-up for at least 2 years, or until collapse progression presented in radiographic examination. The exclusion criteria were as follows: (1) history of surgical treatment of the affected hip, (2) incomplete clinical or imaging data, (3) Hips with advanced stage ONFH at initial visit, including collapse of the femoral head over 2 mm or presentation of osteoarthritis. A total of 155 hips were reviewed, after screening based on eligible criteria, 24 hips were excluded due to lost of follow-up, leaving 131 hips in the final analyses.

All patients with ONFH were recommended with observational, nonoperative management. Restricted weight-bearing were maintained with bilateral crutches for 3 months after diagnosis. Unilateral crutch was then used for another 3 months, allowing gradual weight bearing. Full weight-bearing was allowed when the patient was free of pain. During the course, patients were asked to practice hip abduction training to strengthen muscles of the gluteal region. All patients underwent regular clinical assessments and radiographic evaluations follow-up at 3-months interval.

Radiological evaluation

Plain radiographs of both anteroposterior (AP) and frog leg (FL) views were taken at every visit. Standardized protocols were employed for acquiring all plain radiographs. For the AP view, subjects were positioned supine with legs rotated internally at 15 degrees, aligning the crosshair of the X-ray beam on the pubic symphysis and included both iliac crests within the field of view. For the FL view, patients lay supine with hips flexed to 30 degrees, thighs abducted and externally rotated, ensuring the feet contacted each othe. The X-ray beam directed from anterior to posterior and centered on the pubic symphysis with the pelvic plane being parallel to the table.

Radiographs obtained at the initial visit were used to evaluate the Association Research Circulation Osseous (ARCO) stage of the affected hip. Stage I is defined as abnormalities could only be noted on MRI; stage II is defined as the presence of focal osteosclerosis and osteoporosis on radiographic imaging without collapse of the femoral head; stage IIIA is defined as collapse of the femoral head lesser than 2 mm and demarcating sclerosis along the lesion are noted; stage IIIB is marked by collapse of the femoral head more than 2 mm; stage IV is defined as fragmentation collapse of the femoral head and progression to osteoarthritis [14].

The degree of collapse was evaluated by concentric circles on radiographs of both AP and FL views using Image J software (1.52a, National Institutes of Health, USA) [15, 16]. Collapse progression was defined as the amount of collapse increased by more than 1 mm during the two year follow-up [17] (i.e. from ARCO stage I or II to stage IIIA, or from stage IIIA to stage IIIB) in either AP or FL view.

Table 1 MRI scanning parameters of T1-weighted coronal images

Scanner model	Parameter 1	Parameter 2	Parameter 3	Parameter 4
	SIEMENS Prisma	GE Signa HDxt	GE Signa HDxt	GE Signa HDxt
Magnetic field strength	3.0T	3.0T	3.0T	1.5T
Slice thickness (mm)	3	4	5	5
Spacing between slices (mm)	3.6 or 3.9	4.4 or 4.5	6	6
TR (ms)	500	430–550	350–770	520–960
TE (ms)	10	7–10	7–17	12–14

TR: time of repetition, TE: time of echo

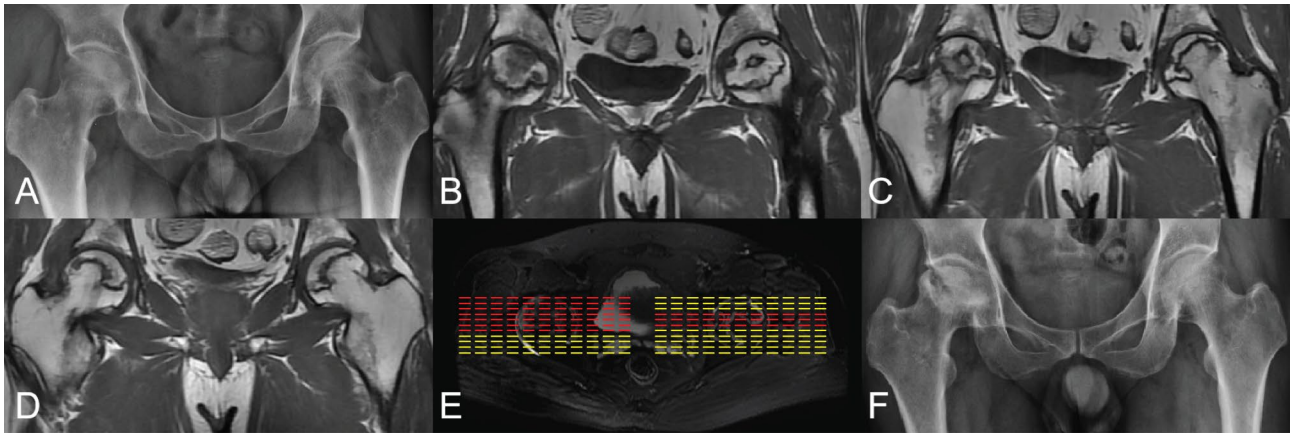

Fig. 1 A Case of bilateral osteonecrosis of the femoral head. A 35 years old male present bilateral hip pain of 2 weeks and received conservative treatment and follow-up. (**A**) X-ray of initial visit showed bilateral ONFH, both hips were classified as JIC type C2. (**B**)-(**C**) Slices of coronal T1 MRI. (**E**) Illustration of lesion involvement: dash lines were slices of femoral head and red lines indicated large lesion slices; the LLR of left hip was 27.27% (3/11), and the LLR of right hip was 63.64% (7/11); (**F**) X-ray of 2 years after initial visit showed right hip experience femoral head collapse progression, while no significant progression was seen in the left hip

MRI evaluation

All hips were diagnosed and evaluated on T1-weighted coronal images at the initial visit. MRI data was acquired using three scanners (Siemens Prisma 3.0 T, GE Signa HDxt 3.0 T, GE Signa HDxt 1.5 T). The coronal T1-weighted turbo spin echo (TSE) images were acquired with scanning parameters set as follows: a range of TR/TE values from 350–960/7–17 ms, and a slice thickness ranging from 3 to 5 mm. Considering slice count may affect the following analysis, we categorized the scanning parameters into four types according to slice thickness and the model of the scanner (Table 1).

The Japanese Investigation Committee (JIC) classification were determined by the mid-coronal slice of T1-weighted MRI. The JIC classification is comprised of four types, including A, B, C1 and C2. ONFH with lesion that was not seen in the central coronal slice was classified as type A [3, 11].

The slice count of femoral head were obtained by examining T1-weighted coronal images, and the total number of slices presenting with femoral head was counted. Slice present with low-intensity band in femoral head were regraded as presence of necrosis. The slice count of large lesion was determined by evaluating every slice with necrosis. Slices present with large lesion extending outside the lateral acetabular edge was regarded as large lesion slice, and the total number of slice with large lesion was counted. The LLR was then calculated as follows: LLR = slice count of large lesion / slice count of femoral head (Fig. 1).

Anterior slices only present with necrosis of femoral head without exposure of the acetabulum were also regraded as large lesion slice, because these slice were located at the most anterior portion of the femoral head without acetabular coverage. Note that the lateral necrotic margin was defined as the lateral boarder of the lesion at the subchondral area (Fig. 2). Identifying the boundary of necrotic lesion in some cases may be difficult due to bone marrow edema. In these cases, images from multiple sequences including T2-weighted fat suppression sequence or contrast-enhanced MRI were also used in combination. The distance between the lateral margin of ONFH lesion and the lateral edge of acetabulum may be too close to distinguish in some slices. We tended to categorize these slices as large lesion slices to avoid underestimating the risk of collapse progression when our results applied in clinical practice.

MRI images from 50 patients were randomly chosen for inter- and intra-observer agreement assessment. Two independent orthopaedics surgeon (WH, ZL) assessed

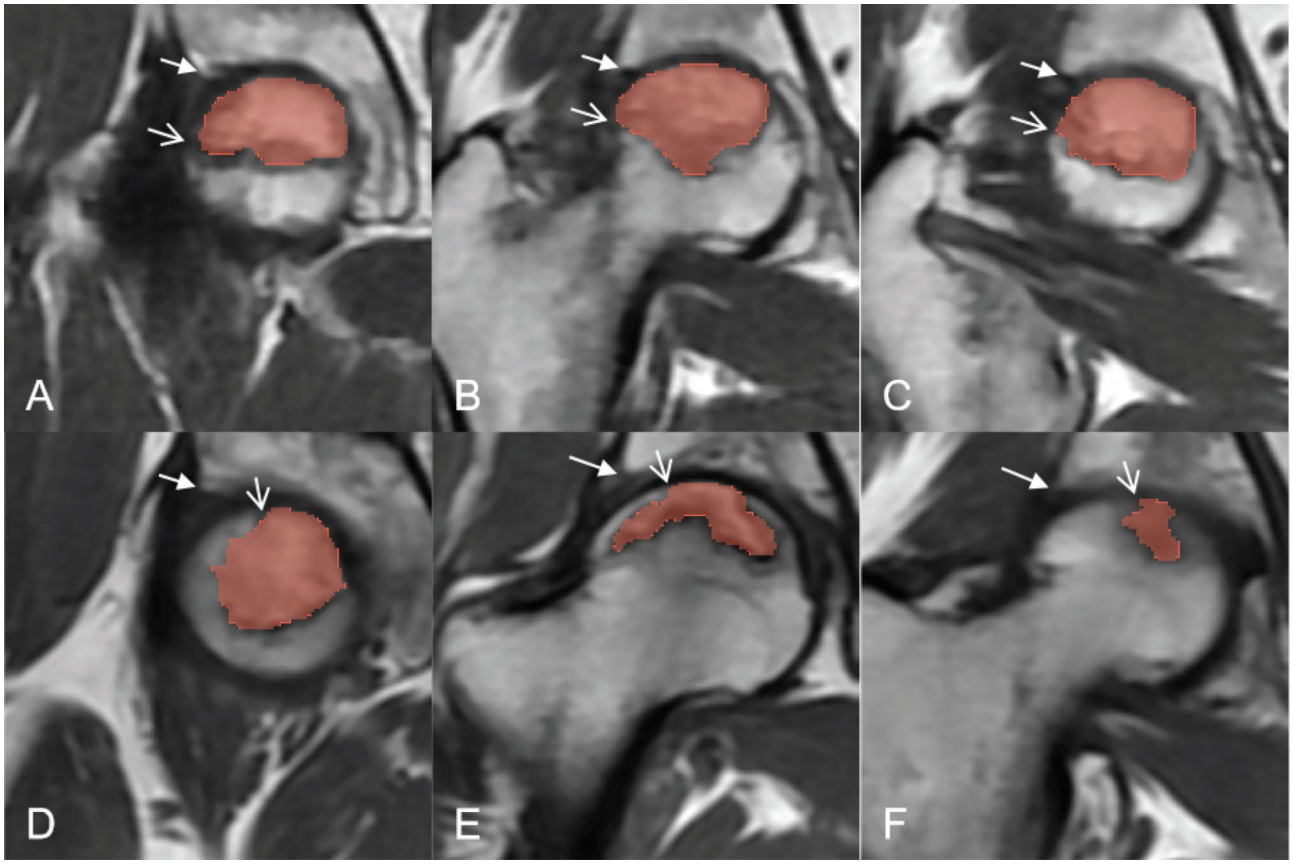

Fig. 2 Illustration of MRI slice evaluation. (**A**), (**B**), and (**C**) are large lesion slices. The lateral margin of necrotic lesion at the subchondral area (simple arrows) extends beyond the lateral edge of the acetabulum (filled arrows). (**D**), (**E**), and (**F**) are slices presents with necrosis, but not large lesion. The lateral margin of necrotic lesion (simple arrows) is medial to the edge of the acetabulum (filled arrows)

the LLR of the patients separately to evaluate the inter-observer reliability. One of the rater (ZL) assessed again 24 h after the initial assessment for intra-observer reliability evaluation. Intraclass correlation coefficient (ICC) was used to evaluate the inter-and intra-observer reliability.

Statistical analysis

Data were reported as medians and inter quartile ranges (IQR) for continuous variables and as percentages or frequencies for categorical variables. Mann-Whitney test or Kruskal-Wallis test was used for continuous variables and chi-square test for categorical variables to estimate the difference among groups. Univariate and multivariate logistic regression analyses were adopted to evaluate the relationship between LLR and collapse progression. Three models were constructed, including univariate model (no covariate was adjusted), model 1 (LLR and ARCO stage were included) and model 2 (age and gender were further adjusted on the basis of model 1). Finally, receiver operating characteristic (ROC) curves were constructed and the area under the curve (AUC) was calculated. All statistical analyses were performed on R studio (R for Windows, version 4.3.2).

Result

The ICC value for inter-observer reliability of LLR was 0.916 ($P<0.001$). For intra-observer reliability, the ICC value was 0.954 ($P<0.001$). Both indicated high reproductibility of LLR.

As shown in Table 2, the percentages of JIC type C2 (52.38%) and ARCO stage IIIA (53.97%) ONFH were significantly higher in the progression group compared to the non-progression group ($P<0.001$, $P=0.007$, respectively). The difference of LLR between two groups were statistically significant ($P<0.001$), with a median of 66.67% (IQR, 44.95–87.86%) LLR in the progression group compared to 25.00% (IQR, 0.00–42.86%) in the non-progression group.

Subgroup analysis was performed based on JIC classification (Table 3). For type A ONFH, none of the hips had lesion extended beyond the coverage of acetabulum, and none of the hip collapsed during follow-up. For type B lesion, the overall median of LLR was 26.79% (IQR, 2.50–40.00%), and there was one hip progressed to collapse of

Table 2 Baseline characteristics of included hips

	Non-progression	Collapse progression	*P*
N	68	63	
Affected side			0.4
Left	35 (51.47%)	38 (60.32%)	
Right	33 (48.53%)	25 (39.68%)	
Age (years)	35.50 [28.75, 47.00]	38.00 [32.50, 46.00]	0.121
Gender			0.127
Male	40 (58.82%)	46 (73.02%)	
Female	28 (41.18%)	17 (26.98%)	
JIC classification			< 0.001
Type A	11 (16.18%)	0 (0.00%)	
Type B	13 (19.12%)	2 (3.17%)	
Type C1	29 (42.65%)	27 (42.86%)	
Type C2	15 (22.06%)	34 (53.97%)	
ARCO			0.007
Stage I	6 (8.82%)	1 (1.59%)	
Stage II	42 (61.76%)	28 (44.44%)	
Stage IIIA	20 (29.41%)	34 (53.97%)	
Etiology			0.36
Steroidal	41 (60.29%)	31 (49.21%)	
Alcoholic	21 (30.88%)	27 (42.86%)	
Idiopathic	6 (8.82%)	5 (7.94%)	
Duration of pain (months)	1.00 [0.00, 7.00]	2.00 [1.00, 5.50]	0.073
LLR (%)	25.00 [0.00, 42.86]	66.67 [44.95, 87.86]	< 0.001

Data are presented as median [IQR] or *n* (%); LLR: large lesion ratio, JIC: Japanese Investigation Committee, ARCO: Association Research Circulation Osseous

Table 3 Comparison of MRI evaluation results in JIC subgroups

		Non-progression	Collapse progression	*P*
A				
	N	11	0	
	LLR(%)	0.00 [0.00, 0.00]	-	-
B				
	N	13	1	
	LLR(%)	28.57 [0.00, 40.00]	20.00	-
C1				
	N	29	28	
	LLR(%)	28.57 [10.00, 50.00]	59.82 [44.81, 93.18]	< 0.001
C2				
	N	15	34	
	LLR(%)	37.50 [6.25, 61.90]	70.00 [50.00, 85.71]	0.002

Data are presented as median [IQR]; LLR: large lesion ratio, JIC: Japanese Investigation Committee

femoral head with a LLR of 20%. For type C1 subgroup, the overall median of LLR was 45.45% (IQR, 28.57–75.00%); and for type C2 subgroup, the overall median of LLR was 63.64% (IQR,40.00–85.71%). Approximately half of the type C1 hips and two thirds of the type C2 hips had collapse progression. In the collapse progression group of type C1 hips, the median of LLR was 59.82% (IQR, 44.81–93.18%), while in the non-progression group, the median of LLR [28.57% (IQR, 10.00–50.00%)] was significantly lower ($P<0.001$). Similarly, LLR was significantly lower in the non-progression group of type C2 hips ($P=0.002$). The median of LLR was 37.50% (IQR, 6.25–61.90%) in the non-progression group of type C2 hips, compared with 70.00% (IQR, 50.00–85.71%) in the collapse progression group.

We further investigate the difference of MRI evaluation results between four scanning parameter groups (Table 4). There was no statistically significant difference in JIC classification and LLR among groups with different scanning parameters ($P=0.547$, $P=0.917$, respectively), indicating that the distribution of ONFH types in four groups was relatively consistent, and most importantly, LLR were not affected by the difference in scanning parameters.

Univariate logistic regression analysis showed significant correlations between LLR (OR, 1.60 [95% CI, 1.36–1.87]; $P<0.001$) with collapse progression. Multivariate regression analysis (model 1) showed that LLR (OR, 1.60 [95% CI, 1.36–1.87]; $P<0.001$) was associated with collapse progression independent to ARCO staging. After further adjusting for age and gender (model 2), LLR (OR, 1.46 [95% CI, 1.24–1.78]; $P<0.001$) still showed a consistent independent correlation with collapse progression, suggesting the result were relatively robust (Table 5).

The predictive efficacy of LLR and JIC classification on the progression of collapse were analyzed by construction of ROC curves and calculation of corresponding AUC values. Results suggested that the predictive efficacy of LLR (AUC=0.84) was higher compared with JIC

Table 4 Comparison of MRI evaluation results grouped by scanning parameters

	Parameter 1	Parameter 2	Parameter 3	Parameter 4	*P*
n	21	41	35	34	
JIC classification					0.547
Type A	4 (19.05%)	5 (12.20%)	4 (11.43%)	4 (11.76%)	
Type B	0 (0.00%)	2 (4.88%)	2 (5.71%)	5 (14.71%)	
Type C1	3 (14.29%)	5 (12.20%)	6 (17.14%)	8 (23.53%)	
Type C2	13 (61.90%)	27 (65.85%)	23 (65.71%)	17 (50.00%)	
Number of large lesion slices	4.00 [3.00, 7.00]	4.00 [1.00, 7.00]	3.00 [2.00, 5.00]	3.50 [1.25, 5.00]	0.240
Number of femoral head slices	11.00 [10.00, 12.00]	10.00 [9.00, 10.00]	7.00 [6.00, 7.00]	7.00 [7.00, 7.00]	< 0.001
LLR (%)	40.00 [25.00, 63.64]	40.00 [10.00, 70.00]	50.00 [28.57, 84.52]	50.00 [21.25, 70.24]	0.917

Data are presented as median [IQR]; LLR: large lesion ratio, JIC: Japanese Investigation Committee

Table 5 Result of univariate and multivariate logistics regression

	Collapse progression					
	Univariate model		Model 1		Model 2	
	OR (95% CI)	*P*	OR (95% CI)	*P*	OR (95% CI)	*P*
LLR (per 10%)	1.60(1.36–1.87)	< 0.001	1.60(1.37–1.93)	< 0.001	1.60(1.36–1.91)	< 0.001

Univariate model: no covariate was adjusted; Model 1: LLR and ARCO stage were included; Model 2: additionally adjusted for age and gender. OR: odds ratio, CI: confidence interval, LLR: large lesion ratio

classification (AUC=0.74). The Youden index was then calculated for different cutoff values of LLR, yielding an optimal threshold of 40%, with a sensitivity of 88.89% and a specificity of 69.12% (Fig. 3).

Discussion

The most important findings of this study was that that LLR was an independent risk factor of collapse progression and may be a more effective tool for the prediction of collapse progression compared to JIC classification. Moreover, it could be applied on MRI images with different scanning parameters. This practical and reproducible method is suitable for risk assessment of collapse progression at initial diagnosis with MRI.

Precisely evaluating the risk of collapse progression of the femoral head is crucial before recommending a treatment regime to an ONFH patient. To achieve this goal, several classification systems have been developed. In the Steinberg system, the size of the lesion is assessed by percentage (<15%, 15–30%, >30%), or calculated using a special software in the revised version [6, 18]. Different from directly measuring the volume of lesion, the Kerboul classification system measures the angle of the lesion involvement on anteroposterior and lateral radiographs, or on mid-coronal and mid-sagittal slices of MRI [12, 19]. The JIC classification is one of the widely used classification system. Sultan et al. reported that compared to both the Steinberg and Kerboul, the JIC classification showed higher intra- and inter- observer agreement [20]. Moreover, JIC classification showed promising prognostic value while maintaining simplicity [3, 20].

In the JIC classification, ONFH lesion with localization at the lateral weight-bearing area is considered more severe [3, 20]. Most of the existing classification systems emphasize on the size or the lateral boundary of ONFH lesion, but multiple studies have suggested that evaluating the anterior portion of the lesion is also important for the prediction of collapse progression [10, 21–24]. Results from the study of Kubo et al. indicated that collapse could develop when the lesion involved the anterior of the femoral head even if the lesion is medially located [23]. Similarly, Nishii et al. pointed out that involvement of the anterosuperior portion of the femoral head was closely correlated with collapse [22].

It has been well established that acetabular coverage of necrotic lesion plays an important part in the progression of ONFH [25, 26]. When the lesion extends beyond the coverage of acetabulum, collapse may occur or progress rapidly due to excessive shearing force between the lateral edge of acetabulum and femoral head. Previous studies [23, 27] have found that necrotic lesion usually accounts for more volume in the anterior portion of femoral head. Moreover, acetabular coverage on the anterior of femoral head is naturally decreased due to acetabular anteversion, making the anterolateral region of the femoral head vulnerable to collapse progression.

Therefore, assessing the necrotic lesion comprehensively is necessary. Recent studies have developed some effective methods to evaluate necrotic lesion on different views of radiographs simultaneously in order to quantify both anterior and lateral involvement [9, 10]. However, in the early stage of ONFH, the boundary of the lesion may

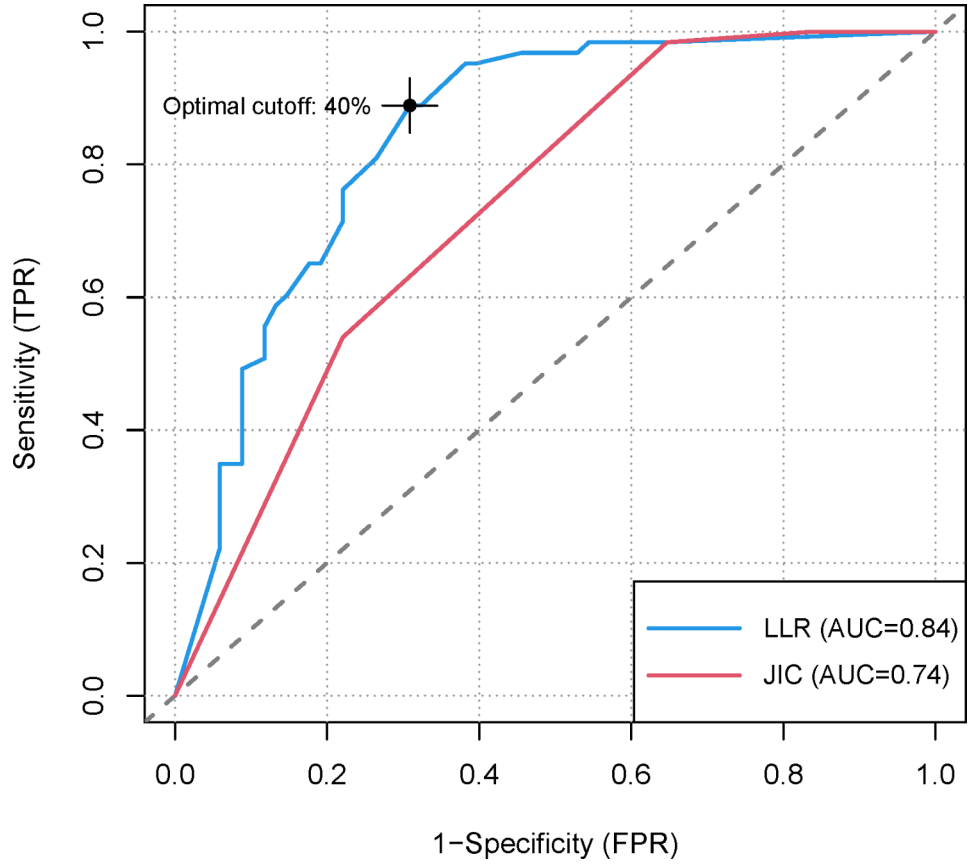

Fig. 3 Receiver operating characteristic curves. The AUC of LLR and JIC were 0.84, and 0.74, respectively. The optimal cutoff point for LLR was 40%, with a sensitivity of 88.89% and a specificity of 69.12%. AUC: area under the curve, LLR: large lesion ratio, JIC: Japanese Investigation Committee

be blurred, which could affect the assessment of radiographs. On the contrary, the boundary of necrotic lesion is relatively clearer on MRI in every stage, especially on T1-weighted images. Moreover, ARCO stage I ONFH could only be assessed through MRI [11].

One of the problem when assessing ONFH on MRI is how to determine the most valuable slice, because the size and location of necrotic lesion across the slices are usually different. In the definition of JIC classification, the mid-coronal slice is chosen [11]. Assessing ONFH on mid-coronal slice alone could be problematic when the larger portion of the necrotic lesion is located in the anterior of the femoral head, because the risk of collapse progression may be underestimated. Similar problem could also occur when trying to use different views for evaluation.

The major improvement of the method introduced in our study was that we evaluate every slice of the coronal view. Because the whole of the necrotic lesion was inspected slice by slice from anterior to posterior, we could assess the anterolateral portion of the femoral head more comprehensively. In the recent version of ARCO classification, when the lateral margin of necrotic lesion extends beyond the lateral edge of the acetabulum, the lesion is categorized as large [28]. Therefore, we were evaluating whether the lesion could be categorized as large lesion on every slice, and further transferred the slice counts into LLR.

In our opinion, LLR may reflect the intactness of the anterolateral portion of femoral head. Biomechanical experiments has confirmed that the anterolateral portion bears most of the pressure on femoral head in daily activities like standing and walking. If the intactness of anterolateral femoral head is compromised by necrotic lesion, collapse progression may occur rapidly [29, 30].

As scanning parameters like slice thickness could significantly affect the slice count of imaging, we used ratios to quantify the necrotic lesion, which was proven to be robust under different scanning parameters according to our results. In addition, comparing the slice count of large lesion or necrosis directly could also be problematic even under unified scanning parameters because of the difference in the size of femoral heads. By transferring slice count to ratio, we believed this evaluating method could be generalize to other institutions.

Therefore, with comprehensive evaluation of the anterolateral portion of the femoral head using LLR, a more accurate identification of patients at high risk of

collapse progression could be achieved, providing useful insight for clinical decision-making. Furthermore, the reproducibility and applicability of LLR across various MRI scanning parameters could ensure uniformity across different healthcare settings.

There are several limitations in the current study. Firstly, due to the nature of retrospective study design, selection bias is inevitable. Secondly, although multivariate regression showed LLR was independently associated with the risk of collapse, there may be factors that were not accounted for, including the amount of physical activity. Finally, there was risk of poor treatment adherence of patients even if they were closely followed up and monitored. Large-scale prospective cohort studies with are needed to further validate our results in the future.

In conclusion, calculating LLR by evaluating every slice of femoral head on MRI may be an effective and robust way to quantify the involvement of necrotic lesion. LLR could served as an efficient tool to assess the risk of collapse progression and guide the selection of treatment strategy.

Abbreviations

ONFH	Osteonecrosis of the femoral head
MRI	Magnetic resonance imaging
LLR	Large Lesion Ratio
STROBE	Strengthening The Reporting of Observational Studies In Epidemiology
AP	Anteroposterior
FL	Frog leg
ARCO	Association Research Circulation Osseous
TSE	T1-weighted turbo spin echo
JIC	Japanese Investigation Committee
ICC	Intraclass correlation coefficient
IQR	Inter quartile ranges
ROC	Receiver operating characteristic
AUC	Area under the curve

Acknowledgements
Not applicable.

Author contributions
(I) Conception and design: SG, WH; (II) Administrative support: WH; (III) Provision of study materials or patients: ZL, WH; (IV) Collection and assembly of data: HZ, MW; (V) Data analysis and interpretation: SG, ZL; (VI) Manuscript writing: All authors; (VII) Final approval of manuscript: All authors.

Funding
This study was funded by Zhongshan Social Welfare and Basic Research Project (Grant Number: 2023B3029) and GuangDong Basic and Applied Basic Research Foundation (2024A1515030134).

Data availability
The data generated and analyzed during the current study are not publicly available to keep privacy of participants and the confidentiality of data, but are available from the corresponding author on reasonable request.

Declarations

Ethics approval and consent to participate
This study was conducted in accordance with the ethical guidelines of the Helsinki Declaration and was approved by the ethics committee of the First Affiliated Hospital of Guangzhou University of Chinese Medicine (JY2023-005), with a waiver for informed consent for retrospective data analysis.

Consent for publication
Not applicable.

Competing interests
The authors declare no competing interests.

Received: 13 November 2023 / Accepted: 16 August 2024
Published online: 16 September 2024

References

1. Zhao DW, Yu M, Hu K, Wang W, Yang L, Wang BJ, Gao XH, Guo YM, Xu YQ, Wei YS, et al. Prevalence of nontraumatic osteonecrosis of the femoral head and its Associated Risk factors in the Chinese Population: results from a nationally Representative Survey. Chin Med J (Engl). 2015;128(21):2843–50.
2. Mont MA, Salem HS, Piuzzi NS, Goodman SB, Jones LC. Nontraumatic osteonecrosis of the femoral head: where do we stand today? A 5-Year update. The Journal of bone and joint surgery. Am Volume. 2020;102(12):1084–99.
3. Kuroda Y, Tanaka T, Miyagawa T, Kawai T, Goto K, Tanaka S, Matsuda S, Akiyama H. Classification of osteonecrosis of the femoral head: who should have surgery? Bone Joint Res. 2019;8(10):451–8.
4. Ando W, Sakai T, Fukushima W, Kaneuji A, Ueshima K, Yamasaki T, Yamamoto T, Nishii T, Sugano N. Japanese Orthopaedic Association 2019 guidelines for osteonecrosis of the femoral head. J Orthop Sci. 2021;26(1):46–68.
5. Shimizu K, Moriya H, Akita T, Sakamoto M, Suguro T. Prediction of collapse with magnetic resonance imaging of avascular necrosis of the femoral head. J Bone Joint Surg Am. 1994;76(2):215–23.
6. Steinberg ME, Bands RE, Parry S, Hoffman E, Chan T, Hartman KM. Does lesion size affect the outcome in avascular necrosis? Clin Orthop Relat Res. 1999(367):262–71.
7. Takashima K, Sakai T, Hamada H, Takao M, Sugano N. Which classification system is most useful for classifying osteonecrosis of the femoral head? Clin Orthop Relat Res. 2018;476(6):1240–9.
8. Takatori Y, Kokubo T, Ninomiya S, Nakamura S, Morimoto S, Kusaba I. Avascular necrosis of the femoral head. Natural history and magnetic resonance imaging. J Bone Joint Surg Br. 1993;75(2):217–21.
9. Fan Y, Zhang J, Chen M, Pang F, Chen H, Wu Y, Liang Y, Wei Z, Cai K, Li W, et al. Diagnostic value of necrotic lesion boundary in bone collapse of femoral head osteonecrosis. Int Orthop. 2022;46(3):423–31.
10. Wei QS, Li ZQ, Hong ZN, Hong GJ, Pang FX, Yang P, Yang F, Yuan YJ, Zhuang ZK, He W. Predicting Collapse in Osteonecrosis of the femoral Head using a New Method: preserved angles of anterior and lateral femoral head. J Bone Joint Surg Am. 2022;104(Suppl 2):47–53.
11. Sugano N, Atsumi T, Ohzono K, Kubo T, Hotokebuchi T, Takaoka K. The 2001 revised criteria for diagnosis, classification, and staging of idiopathic osteonecrosis of the femoral head. J Orthop Sci. 2002;7(5):601–5.
12. Kerboul M, Thomine J, Postel M, Merle DR. The conservative surgical treatment of idiopathic aseptic necrosis of the femoral head. J Bone Joint Surg Br. 1974;56(2):291–6.
13. Koo KH, Kim R. Quantifying the extent of osteonecrosis of the femoral head. A new method using MRI. J Bone Joint Surg Br. 1995;77(6):875–80.
14. Yoon BH, Mont MA, Koo KH, Chen CH, Cheng EY, Cui Q, Drescher W, Gangji V, Goodman SB, Ha YC, et al. The 2019 Revised Version of Association Research Circulation Osseous Staging System of Osteonecrosis of the femoral head. J Arthroplasty. 2020;35(4):933–40.
15. Bomer J, Klerx-Melis F, Holscher HC. Painful paediatric hip: frog-leg lateral view only! Eur Radiol. 2014;24(3):703–8.
16. Petek D, Hannouche D, Suva D. Osteonecrosis of the femoral head: pathophysiology and current concepts of treatment. EFORT Open Rev. 2019;4(3):85–97.
17. Nishii T, Sugano N, Ohzono K, Sakai T, Haraguchi K, Yoshikawa H. Progression and cessation of collapse in osteonecrosis of the femoral head. Clin Orthop Relat Res. 2002(400):149–57.
18. Steinberg DR, Steinberg ME, Garino JP, Dalinka M, Udupa JK. Determining lesion size in osteonecrosis of the femoral head. J Bone Joint Surg Am. 2006;88(Suppl 3):27–34.
19. Ha YC, Jung WH, Kim JR, Seong NH, Kim SY, Koo KH. Prediction of collapse in femoral head osteonecrosis: a modified Kerboul method with use of magnetic resonance images. J Bone Joint Surg Am. 2006;88(Suppl 3):35–40.

20. Sultan AA, Mohamed N, Samuel LT, Chughtai M, Sodhi N, Krebs VE, Stearns KL, Molloy RM, Mont MA. Classification systems of hip osteonecrosis: an updated review. Int Orthop. 2019;43(5):1089–95.
21. Kang JS, Moon KH, Kwon DG, Shin BK, Woo MS. The natural history of asymptomatic osteonecrosis of the femoral head. Int Orthop. 2013;37(3):379–84.
22. Nishii T, Sugano N, Ohzono K, Sakai T, Sato Y, Yoshikawa H. Significance of lesion size and location in the prediction of collapse of osteonecrosis of the femoral head: a new three-dimensional quantification using magnetic resonance imaging. J Orthop Res. 2002;20(1):130–6.
23. Kubo Y, Motomura G, Ikemura S, Sonoda K, Hatanaka H, Utsunomiya T, Baba S, Nakashima Y. The effect of the anterior boundary of necrotic lesion on the occurrence of collapse in osteonecrosis of the femoral head. Int Orthop. 2018;42(7):1449–55.
24. Ohzono K, Saito M, Takaoka K, Ono K, Saito S, Nishina T, Kadowaki T. Natural history of nontraumatic avascular necrosis of the femoral head. J Bone Joint Surg Br. 1991;73(1):68–72.
25. Hipp JA, Sugano N, Millis MB, Murphy SB. Planning acetabular redirection osteotomies based on joint contact pressures. Clin Orthop Relat Res. 1999(364):134–43.
26. Nozawa M, Enomoto F, Shitoto K, Matsuda K, Maezawa K, Kurosawa H. Rotational acetabular osteotomy for osteonecrosis with collapse of the femoral head in young patients. J Bone Joint Surg Am. 2005;87(3):514–20.
27. Yang F, Deng X, Xin P, Hong Z, Pang F, He W, Wei Q, Li Z. The value of the Frog lateral view radiograph for detecting collapse of Femur Head Necrosis: a retrospective study of 1001 cases. Front Med (Lausanne). 2022;9:811644.
28. Koo KH, Mont MA, Cui Q, Hines JT, Yoon BH, Novicoff WM, Lee YJ, Cheng EY, Drescher W, Hernigou P, et al. The 2021 Association Research Circulation Osseous classification for early-stage osteonecrosis of the femoral head to computed tomography-based study. J Arthroplasty. 2022;37(6):1074–82.
29. Genda E, Iwasaki N, Li G, Macwilliams BA, Barrance PJ, Chao EY. Normal hip joint contact pressure distribution in single-leg standing–effect of gender and anatomic parameters. J Biomech. 2001;34(7):895–905.
30. Yoshida H, Faust A, Wilckens J, Kitagawa M, Fetto J, Chao EY. Three-dimensional dynamic hip contact area and pressure distribution during activities of daily living. J Biomech. 2006;39(11):1996–2004.

Publisher's note